Electronic structures of solid BC_{59}

Yoshiyuki Miyamoto
Microelectronics Research Laboratories, NEC Corporation, 34 Miyukigaoka, Tsukuba 305, Japan

Noriaki Hamada
Fundamental Research Laboratories, NEC Corporation, 34 Miyukigaoka, Tsukuba 305, Japan

Atsushi Oshiyama
Microelectronics Research Laboratories, NEC Corporation, 34 Miyukigaoka, Tsukuba 305, Japan

Susumu Saito
Fundamental Research Laboratories, NEC Corporation, 34 Miyukigaoka, Tsukuba 305, Japan
(Received 18 February 1992)

We have investigated the cohesion and electronic structures of a metallic fullerene consisting of a single boron-substituted C_{60} (BC_{59}) molecule by performing a first-principles total-energy band-structure calculation. We have found that BC_{59} fullerenes are condensed exothermically and that a boron-induced metallic band appears above the valence bands of pristine C_{60}. We have also found that the boron-induced state has the character of an acceptor state, indicating that substitutional BC_{59} in solid C_{60} may act as an "acceptor fullerene." The dispersion and the width of the boron-induced band have been found to be sensitive to the rotation of the fullerene.

I. INTRODUCTION

Electron doping in solid C_{60} has been achieved with alkali-metal atoms inserted at the interstitial sites[1] and superconductivity has been discovered in the alkali-metal fullerides, A_xC_{60} (A = K, Rb, and Cs).[2-5] Theoretical studies within the local-density approximation (LDA) have revealed that an electron transfer occurs from alkali-metal s orbitals to conduction bands of solid C_{60} and that injected electrons in the conduction bands play an important role in the superconductivity.[6-9] The success of the electron doping is due to the large electronegativity of C_{60}.

Hole doping has now become the next target for the material design of fullerenes. The electronic structure of hole-introduced solid C_{60} is a matter of fundamental interest. However, hole doping has not yet been achieved in solid C_{60}. Although halogens have been candidates for acceptors in solid C_{60}, a recent theoretical work[10] reveals that the large electronegativity of C_{60} forbids electron transfer from C_{60} to bromine atoms. This situation is considerably different from the case of the graphite intercalation compounds.[11]

Recently, Guo, Jin, and Smalley[12] have succeeded in substituting carbon atoms with boron and nitrogen atoms in cage structures of C_{50}, C_{60}, and C_{70} fullerenes by laser-stimulated vaporization of a composite disk of graphite and boron nitride. The synthesis of B-substituted C_{60} fullerene (BC_{59}) is expected to be a promising way of hole doping in solid fullerenes. However, it is still unknown whether BC_{59} is condensed and what may be the resulting electronic structure of solid BC_{59}.

In this paper, we report our theoretical investigation of the cohesion and electronic structures of solid BC_{59}. We have performed a first-principles total-energy calculation within the LDA. First, we adopted the same crystal structure and the same orientation of the fullerene as those of the face-centered-cubic (fcc) C_{60}.[6] We have found that BC_{59} fullerenes condense with cohesive energy of about 1.8 eV per BC_{59} in this geometry. We have also found that a half-filled band appears above the valence bands of pristine C_{60}. The width of the band is about 0.3 eV and its wave function is extended on the spheroid-shaped cage with large amplitude on the B atom and its neighboring C atoms. From the obtained level location and the feature of the wave function, we have concluded that the boron-induced state has the character of an acceptor state. Next, we have rotated the BC_{59} fullerene 45° with respect to the ⟨001⟩ crystallographic axis and then calculated the electronic structure. We have found that the boron-induced band widens from 0.3 to 0.5 eV upon rotation.

This paper is organized as follows: In Sec. II, the method of the present calculation is described. In Sec. III, the results for the cohesion and the electronic structures of solid BC_{59} are presented, and in Sec. IV the influence of the rotation of the fullerenes on the electronic structures is reported. The conclusion is given in Sec. V.

II. CALCULATION

We perform the first-principles total-energy and band-structure calculation within the framework of the LDA. In the calculation, we use the norm-conserving nonlocal pseudopotentials[13] and a Gaussian-orbital basis set. Two

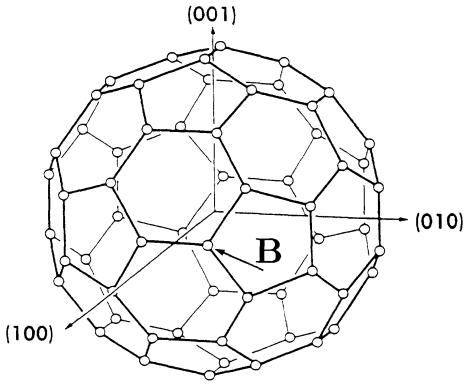

FIG. 1. Atomic geometry of fcc BC_{59}. An arrow denotes the substituted B atom. Only a mirror symmetry with respect to the (001) plane exits.

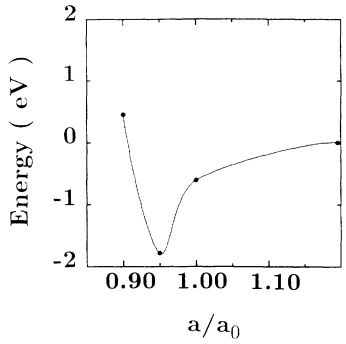

FIG. 2. Calculated total energy in the geometry of Fig. 1 as a function of the lattice constant ($a_0 = 14.2$ Å.)

exponents are assigned for the s and p orbitals of a C atom, which are 0.299 and 2.908 a.u.$^{-2}$ for s and 0.362 and 2.372 a.u.$^{-2}$ for p, respectively. Meanwhile, three and two exponents are assigned for the B s and p orbitals, which are 0.13, 0.75, and 0.82 a.u.$^{-2}$ for s and 0.20 and 1.60 a.u.$^{-2}$ for p, respectively. All of these exponents are determined by fitting them to atomic pseudo-wavefunctions obtained by numerical calculations of isolated C and B atoms. The analytic form[14] of the numerical results of Ceperley and Alder[15] for the exchange-correlation energy is used.

There are two C-C bond lengths in the C_{60} cage, i.e., 1.46 Å on pentagons and 1.40 Å on neighboring hexagons. As for the structure of the BC_{59} fullerene, we assume the same geometry as that of the C_{60} fullerene. Since C_{60} can exothermically solidify with a fcc crystal structure, we expect that BC_{59} can also solidify with a fcc form. We lay a B-C bond in a fcc (001) plane so that the system has a mirror symmetry with respect to the plane, as is shown in Fig. 1. The irreducible Brillouin zone is a quarter of the whole zone.

The band-structure and the total-energy calculation is carried out in the following two cases. In the first case, we choose the azimuthal orientation of BC_{59} with a center of the B-C bond crossing the fcc ⟨100⟩ crystallographic axis, as is shown in Fig. 1. In the next case, we rotate the BC_{59} fullerene 45° around the fcc ⟨001⟩ axis. The mirror symmetry still remains after the 45° rotation. In both cases, we use 4 **k** points per irreducible Brillouin zone during iterations of the self-consistent calculation. The interval of the mesh of the fast Fourier transformation is set to be 0.30 a.u.

III. COHESION AND AN ELECTRONIC STRUCTURE OF SOLID BC_{59}

We first show our results for solid BC_{59} with an atomic geometry shown in Fig. 1. We have calculated the total energies of the solid BC_{59} with changing lattice constant a under the condition of fixing the shape and the orientation of the BC_{59} fullerene. Figure 2 shows calculated total energies as a function of the lattice constant. The a_0 is the experimental lattice constant of pure fcc C_{60} obtained by Fleming *et al.*,[16] $a_0 = 14.2$ Å. The total energy has a minimum when $a = 0.95a_0$; we call it $a_{\min}$ hereafter. The cohesive energy has been estimated to be about 1.8 eV per BC_{59}. The cohesive energy and a feature of the total-energy curve are similar to those of fcc C_{60},[6] i.e., the C_{60} cluster has a closed-shell electronic structure and is condensed via the van der Waals–like interactions. Although the BC_{59} fullerene has an open-shell electronic structure with odd-number electrons, in contrast with the C_{60} fullerene, the present calculation shows that the cohesive energy of solid BC_{59} is of similar magnitude to that of solid C_{60}.

In order to investigate the electronic structure, we have calculated the density of states (DOS) of the fcc BC_{59} both at $a = a_{\min}$ and a_0 and found that the features of the DOS are qualitatively the same in both lattice constants. In this paper we show the calculated DOS at $a = a_0$. In order to interpolate the eigenvalues in the momentum space, we have chosen 10 **k** points per irreducible Brillouin zone as sampling points. The calculated DOS has been broadened with 0.05 eV Gaussian width. The DOS, which is shown in Fig. 3(a), exhibits a similar structure to that of fcc C_{60} (Ref. 6) in the whole energy region except for the vicinity of the Fermi level (E_F). A new peak appears above the valence band, and E_F is located at the center of the peak, i.e., about 0.2 eV above the valence-band top. This new peak is a boron-induced half-filled band. The bandwidth of this new state is about 0.3 eV. Note that there is a mixing between this boron-induced band and the valence band. The relative energy of the center of the boron-induced band from the valence-band top of pristine C_{60} is about 0.2 eV.

We next show the spatial distribution of the wave function of the boron-induced state. Figure 3(b) is a charge-density map of the boron-induced state on the (001) plane. The wave functions in the energy range from $E_F - 0.1$ eV to E_F have been taken into account for drawing the map. Three C atoms and one B atoms are on the plane and are denoted by arrows. The remaining C atoms are located out of the plane, above and below vertices of dotted lines. We note that there is considerable charge distribution on all π orbitals, not only in plane but also at the out-of-plane sites, as can be guessed from the

considerable charge distribution on the opposite side from the boron substituted site. The boron-induced state is thus extended over the whole surface of the spheroid-shaped cage. The bandwidth of 0.3 eV and the overlap with the valence bands shown in Fig. 3(a) are results of the extended character of this state. It can also be seen from Fig. 3 that the amplitude of the wave function of the boron-induced state is slightly weighted toward the π orbitals of the B and neighboring C atoms. The amplitudes of the π orbitals of neighboring C atoms have been found to be bigger than those of the B atoms. We have also calculated the charge-density map of empty states from E_F to $E_F+0.1$ eV, and found that the neighboring C π orbitals also have bigger amplitudes than that of the B atom. The boron-induced state is made by a hybridization of π orbitals on the hollow cage, which come from $2p$ atomic orbitals of B and C atoms. The hybridization results in bonding and antibonding π orbitals. Since the B $2p$ orbital has a much higher energy than the C $2p$ orbital, the bonding π orbital has large C $2p$ components, while the antibonding π orbital has large B $2p$ components. A corresponding schematic diagram is shown in Fig. 4, in which the level locations of conduction and valence bands are also shown for comparison. As has been mentioned before, a boron-induced band appears above the valence band, and has large C $2p$ components. Such character in the wave function is similar to that of acceptors in ordinary semiconductors. We expect that the substitutional doping of BC_{59} into solid C_{60} induces an acceptor state and that BC_{59} doping is a more promising way of hole doping in solid C_{60} than halogen doping, which causes a halogen-induced midgap state.[10]

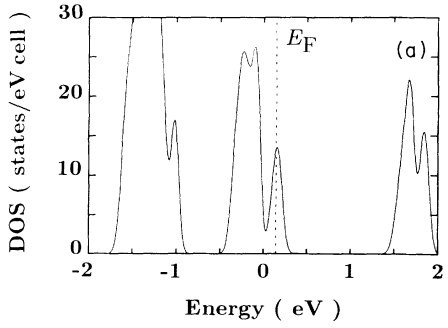

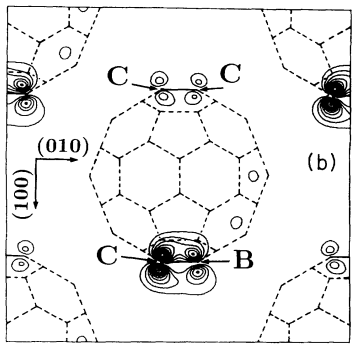

FIG. 3. (a) Density of states of fcc BC_{59} with the geometry of Fig. 1. The dotted line indicates the Fermi level. (b) Charge contour map of the boron-induced level in the (001) plane of the fcc crystal. The contribution of the wave functions in the energy range from $E_F-0.1$ eV to E_F has been included. (The contour map of the wave function from E_F to $E_F+0.1$ eV is similar to this figure.) The density difference between the neighboring contours is 1.44×10^{-3}. The lowest one is 1.44×10^{-3}, the highest is 1.44×10^{-2}. (Here the exhibited charge density is normalized so that the integration over the unit cell gives one.) Arrows indicate three C atoms and one B atom which are located in the (001) plane. Other C atoms are out of this plane, and are located above and below the vertices of the dotted lines.

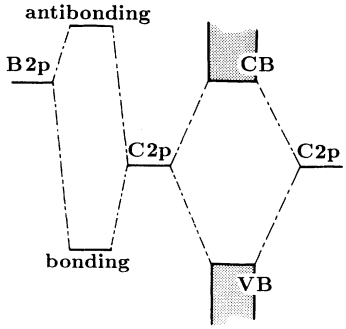

FIG. 4. A schematic diagram for the level location of the boron-induced π state, which is derived by hybridization of mainly $2p$ atomic states of B and C atoms. The valence and conduction bands of solid C_{60} are also shown for the comparison, which are the result of the hybridization of $2p$ orbitals of neighboring C atoms.

IV. INFLUENCE OF A ROTATION OF FULLERENES

We have now shown the stability and electronic structure of the solid BC_{59} in the geometry shown in Fig. 1. Although it has been found that BC_{59} fullerenes are condensed exothermically, there may be more favorable orientations for BC_{59} even within the fcc structure. An anisotropic shape of the wave function of the boron-induced state, which is described in the previous section, suggests that a rotation of fullerenes modifies the band dispersion. We next show our investigation of the influence of the rotation on the electronic structure.

We have rotated the BC_{59} fullerene 45° clockwise with respect to the $\langle 00\bar{1} \rangle$ direction from the geometry shown in Fig. 3(b) and then calculated the total energy and the band structure. The calculations have been done both at $a=a_{\min}$ and $a=a_0$. Without the rotation, the calculated total energies differ by 1.17 eV per BC_{59} between these two lattice constants. The 45° rotation increases the total energy less than a tenth of the above value in both lattice constants. We do not know yet whether this rotating angle gives a metastable geometry of solid BC_{59}. It is, however, worthwhile to investigate the influence of the 45° rotation of fullerenes on the electronic structure. Our calculation with the 45° rotation gives a typical example of the influence of the rotation on the band structures in solid fullerenes.

We have found that the rotation causes considerable

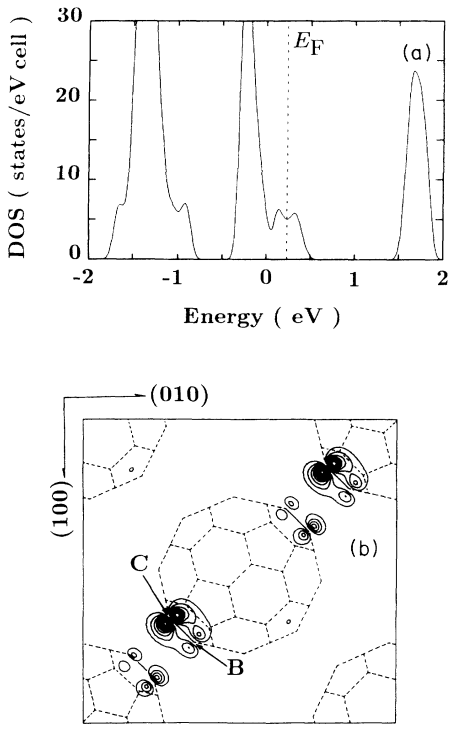

FIG. 5. (a) Density of states of fcc BC_{59} after the 45° clockwise rotation of BC_{59} fullerenes with respect to the $\langle 00\bar{1} \rangle$ direction from the geometry in Fig. 3(b). (b) Charge contour map of boron-induced state in the (001) plane of the fcc crystal. The contribution of the wave function in the energy range from $E_F - 0.1$ eV to E_F has been included. The density difference between neighboring contours is 0.46×10^{-3}. The lowest one is 0.46×10^{-3}, the highest is 0.46×10^{-2}. (Here the exhibited charge density is normalized so that the integration over the unit cell gives one.)

change on the band structure of solid BC_{59}. Figures 5(a) and 5(b) show the DOS in the rotated geometry at $a = a_0$ and the charge-density map of the boron-induced state, respectively. Comparing Fig. 5(a) with Fig. 3(a), we note that the DOS is modified in the whole energy region after the 45° rotation of the BC_{59} fullerenes. A fullerene rotation in solid C_{60} has already been found to occur even at room temperature,[17] and the band variation upon rotation will become an important subject in physics of solid fullerenes.

Now, let us focus our attention on the change of the boron-induced state upon rotation. A sharp peak of the boron-induced band in Fig. 3(a) splits into two broad peaks upon rotation, and then the position of the E_F is in the center of the two peaks. The bandwidth of the boron-induced state increased from 0.3 to 0.5 eV. This boron-induced band is still half-filled. We have investigated the band dispersion of the boron-induced band and have found that the dispersion in the $\langle 1\bar{1}0 \rangle$ direction is larger than that in the $\langle 110 \rangle$ direction. As is shown in Fig. 5(b), the wave function of this state still has a large amplitude around the B-C bond on the spheroid-shaped cage. In the 45° rotated geometry, the center of the B-C bond crosses the $\langle 1\bar{1}0 \rangle$ axis and then the distance between the B-substituted site and the neighboring fullerene decreases. The transfer matrix of electrons in this direction therefore becomes bigger than those in other directions. This orientation thus causes the larger band dispersion in the $\langle 1\bar{1}0 \rangle$ direction than that in the $\langle 110 \rangle$ direction. We have also found that the band dispersion in this direction is also larger than those in the $\langle 1\bar{1}1 \rangle$ and $\langle 111 \rangle$ directions. We therefore expect that the boron-induced band has much larger dispersion in the $\langle 1\bar{1}0 \rangle$ direction than in other directions in momentum space. Such anisotropic character is the reason why two broad peaks appear in the DOS of the 45° rotated geometry of solid BC_{59}. If the boron-induced band had a complete one-dimensional dispersion in the direction, the DOS would have two sharp peaks at the top and bottom of the band.

In contrast to ordinary metals, the metallic fullerenes have a unique internal hollow-cage structure, so that the rotation of each fullerene causes a drastic change of dispersions of the metallic band. Guo, Jin and Smalley[12] have also succeeded in synthesizing nitrogen-substituted C_{60} ($C_{59}N$). We expect, by analogy with solid BC_{59}, solid $C_{59}N$ to have a metallic band of nitrogen-induced state and that its band dispersion is sensitive to the $C_{59}N$ rotation.

V. CONCLUSION

We have investigated the cohesion and the electronic structures of solid BC_{59} by performing a first-principles total-energy band-structure calculation. Although solid BC_{59} has not yet been synthesized, we have shown that BC_{59} fullerenes condense exothermically. A metallic band of the boron-induced state has appeared and its wave function has an anisotropic shape on the hollow-cage structure. The location of the energy level and the feature of the wave function of the boron-induced state are similar to those of acceptor states in ordinary semiconductors. The anisotropic shape of the wave function of the boron-induced state causes the variation of the band dispersion by BC_{59} rotation in solid BC_{59}. This peculiar property of a metallic band comes from the internal hollow-cage structure. Finally, we predict that substitutional BC_{59} in solid C_{60} may behave as an acceptor. BC_{59} doping in pristine C_{60} is a rather promising method of hole doping in solid C_{60}

ACKNOWLEDGMENTS

We would like to thank S. Sawada, M. Saito, and O. Sugino for fruitful discussions.

[1]R. C. Haddon *et al.*, Nature (London) **350**, 320 (1991).
[2]A. Hebard *et al.*, Nature (London) **350**, 600 (1991).
[3]M. J. Rosseinsky *et al.*, Phys. Rev. Lett. **66**, 2830 (1991).
[4]K. Holczer, *et al.*, Science **252**, 1154 (1991).
[5]K. Tanigaki *et al.*, Nature (London) **352**, 222 (1991).
[6]S. Saito and A. Oshiyama, Phys. Rev. Lett. **66**, 2637 (1991).
[7]S. Saito and A. Oshiyama, Phys. Rev. B **44**, 11 536 (1991).
[8]N. Hamada, S. Saito, Y, Miyamoto, and A. Oshiyama, Jpn. J.

Appl. Phys. **30**, L2036 (1991).
[9]A. Oshiyama and S. Saito, Solid State Commun. **82**, 41 (1992).
[10]Y. Miyamoto, A. Oshiyama, and S. Saito, Solid State Commun. **82**, 437 (1992).
[11]For a review, see J. Fisher and T. E. Thompson, Phys. Today **31** (7), 36 (1978); H. Kamimura, *ibid.* **40** (12), 64 (1987).
[12]T. Guo, C. Jin, and R. E. Smalley, J. Phys. Chem. **95**, 4948 (1991).
[13]D. R.Hamann, M. Schlüter, and C. Chiang, Phys. Rev. Lett. **43**, 1494 (1979).
[14]J. Perdew and A. Zunger, Phys. Rev. B **23**, 5048 (1981).
[15]D. M. Ceperley and B. J. Alder, Phys. Rev. Lett. **45**, 566 (1980).
[16]R. M. Fleming *et al.*, in *Clusters and Cluster-Assembled Materials,* edited by R. S. Averback, J. Bernholc, and D. L. Nelson, MRS Symposia Proceedings No. 206 (Materials Research Society, Pittsburgh, 1991), p. 115.
[17]C. S. Yannoni, *et al.*, J. Phys. Chem. **95**, 9 (1991).

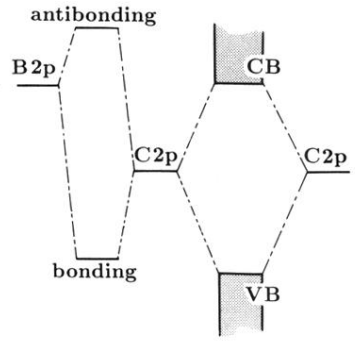

FIG. 4. A schematic diagram for the level location of the boron-induced π state, which is derived by hybridization of mainly $2p$ atomic states of B and C atoms. The valence and conduction bands of solid C_{60} are also shown for the comparison, which are the result of the hybridization of $2p$ orbitals of neighboring C atoms.